

1N-05
11700
P 15

NASA Technical Memorandum 101735

Buffet Induced Structural/Flight-Control System Interaction of the X-29A Aircraft

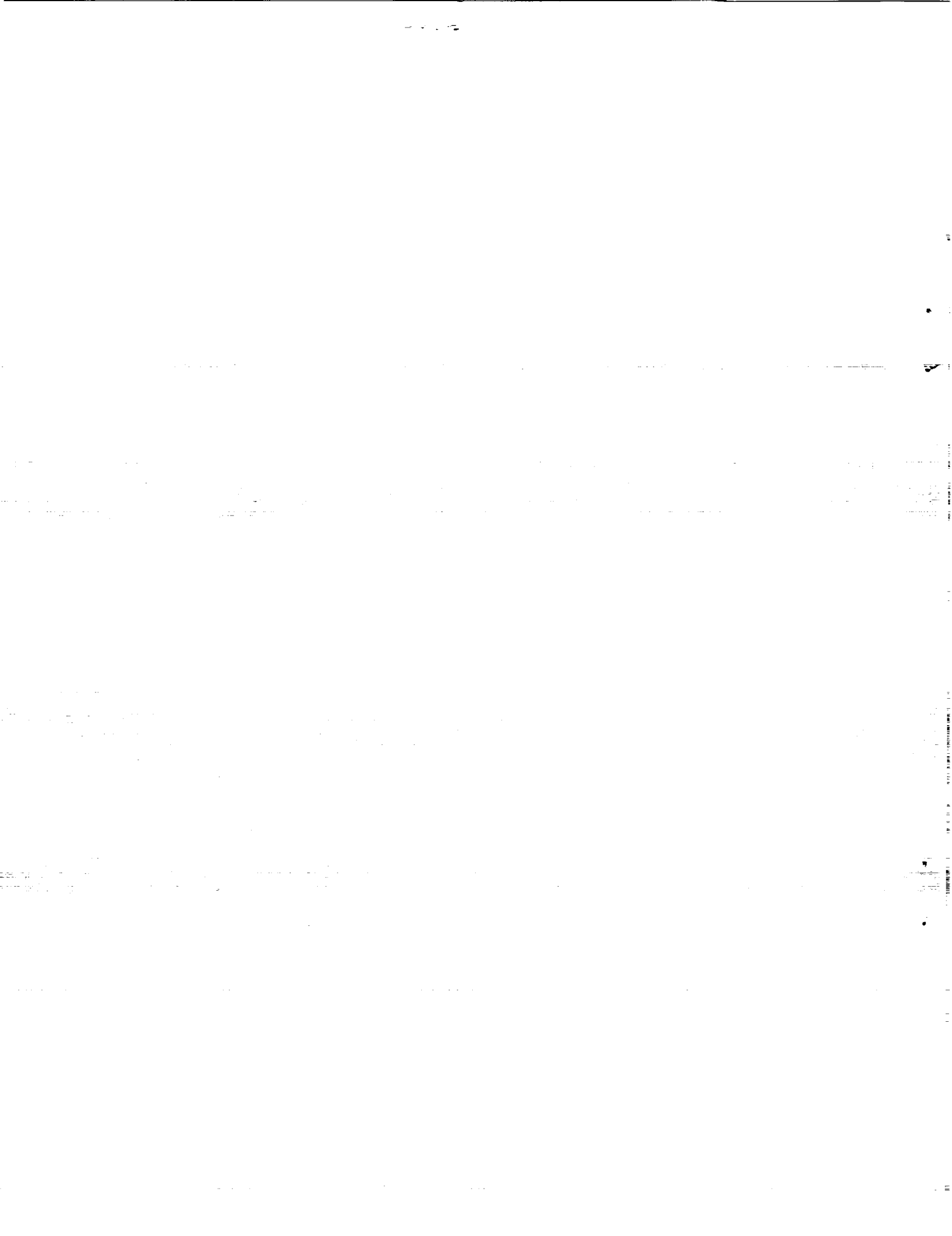
David F. Voracek and Robert Clarke

(NASA-TM-101735) BUFFET INDUCED
STRUCTURAL/FLIGHT-CONTROL SYSTEM INTERACTION
OF THE X-29A AIRCRAFT (NASA) 15 p CSCL 01C

N91-23133

Unclas
G3/05 0011700

April 1991



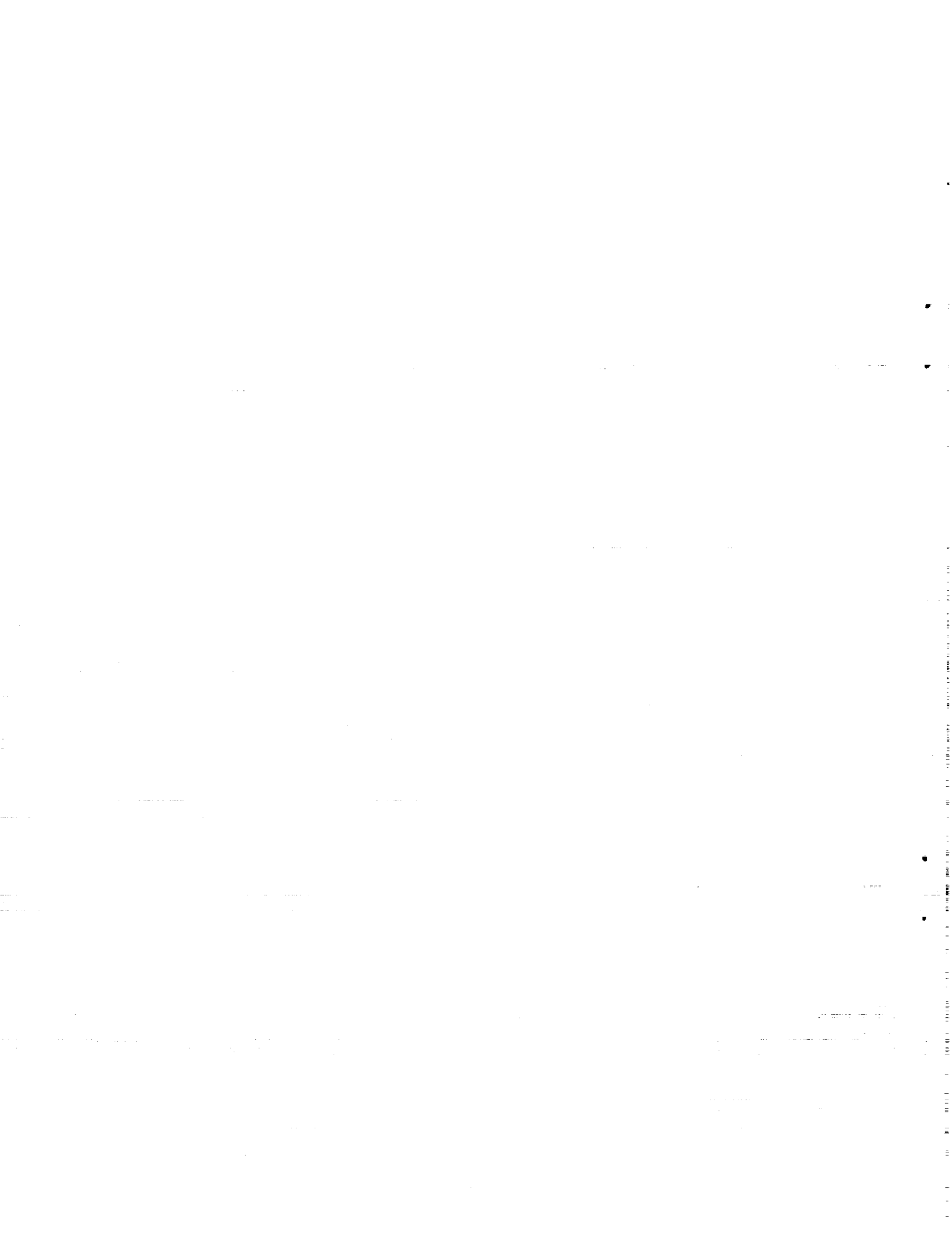
Buffet Induced Structural/Flight- Control System Interaction of the X-29A Aircraft

David F. Voracek and Robert Clarke
Dryden Flight Research Facility, Edwards, California

1991



National Aeronautics and
Space Administration
Dryden Flight Research Facility
Edwards, California 93523-0273



BUFFET INDUCED STRUCTURAL/FLIGHT-CONTROL SYSTEM INTERACTION OF THE X-29A AIRCRAFT

David F. Voracek*

Robert Clarke*

NASA Ames Research Center
Dryden Flight Research Facility
Edwards, California

Abstract

High-angle-of-attack flight regime research is currently being conducted for modern fighter aircraft at the NASA Ames Research Center's Dryden Flight Research Facility. This flight regime provides enhanced maneuverability to fighter pilots in combat situations. Flight research data are being acquired to compare and validate advanced computational fluid dynamic solutions and wind-tunnel models. High-angle-of-attack flight creates unique aerodynamic phenomena including wing rock and buffet on the airframe. These phenomena increase the level of excitation of the structural modes, especially on the vertical and horizontal stabilizers. With high gain digital flight-control systems, this structural response may result in an aeroservoelastic interaction.

A structural interaction on the X-29A aircraft was observed during high-angle-of-attack flight testing. The roll and yaw rate gyros sensed the aircraft's structural modes at 11, 13, and 16 Hz. The rate gyro output signals were then amplified through the flight-control laws and sent as commands to the flaperons and rudder. The flight data indicated that as the angle of attack increased, the amplitude of the buffet on the vertical stabilizer increased, which resulted in more excitation to the structural modes. The flight-control system sensors and command signals showed this increase in modal power at the structural frequencies up to 30° angle of attack. Beyond 30° angle of attack, the vertical sta-

bilizer response, the feedback sensor amplitude, and control surface command signal amplitude remained relatively constant. Data are presented that show the increased modal power in the aircraft structural accelerometers, the feedback sensors, and the command signals as a function of angle of attack. This structural interaction is traced from the aerodynamic buffet to the flight-control surfaces.

Nomenclature

| | |
|----------|---|
| ASE | aeroservoelastic |
| FCC | flight-control computer |
| FCS | flight-control system |
| FFT | fast Fourier transform |
| Hz | Hertz |
| h | altitude, ft |
| ISA | integrated servo actuator |
| M | Mach number |
| NASA | National Aeronautics and Space Administration |
| PSDs | power spectral densities |
| T | sampling time |
| α | angle of attack, deg |

Introduction

The trend of today's aircraft design is toward more flexible, structurally efficient aircraft with high gain flight-control systems. This trend has led to increasing occurrences of the flight-control system dynamics interacting with the aeroelastic response of the aircraft and the emergence of a relatively new discipline called aeroservoelasticity (ASE).¹ These interactions involve

*Aerospace Engineer. Members AIAA

Copyright ©1991 by the American Institute of Aeronautics and Astronautics Inc. No copyright is asserted in the United States under Title 17, U.S. Code. The U.S. Government has a royalty-free license to exercise all rights under the copyright claimed herein for Governmental purposes. All other rights are reserved by the copyright owner.

the unsteady aerodynamics, the flight-control system, and the structural dynamics of an aircraft. In mild cases these interactions can increase dynamic loads on the flight-control surfaces, cause additional fatigue cycles on critical structure, or lead to unforeseen flight control system anomalies with feedback sensors and redundancy management schemes. In more severe cases these ASE interactions can lead to a limited amplitude oscillation or an ASE instability.

Improved test methods and analytical tools have been developed to better understand, predict, and prevent ASE interactions and instabilities.^{2,3,4} The accuracy of the results from these analytical methods depend on a number of modeling details that are difficult to define and predict. Consequently, ASE interactions and instabilities have been encountered in flight that were not predicted through such analysis.^{5,6,7}

The X-29A forward-swept wing aircraft uses a high gain digital flight-control system. Its current flight-test program at the NASA Ames-Dryden Flight Research Facility explores the high-angle-of-attack flight regime. During flight envelope expansion up through 45° angle of attack, an ASE interaction was observed between the buffet on the aircraft, the structural modal response, and the flight-control system in the lateral-directional axis. The small motion of the control surfaces caused by the ASE interaction did not sustain or cause a limited amplitude oscillation. The interaction was caused by an unsteady aerodynamic phenomenon called buffet exciting the aircraft at its modal frequencies. This interaction during higher speed maneuvers played a part in the control surface actuator commands miscomparing in an actuator's hydraulic logic. This miscomparison resulted in the actuator reconfiguration during flight. The actuator reconfiguration caused an increase in flight-test time caused by requirements for repeat flight maneuvers and was one of the catalysts for control law and hardware design changes in the flight-control system.

Aircraft Description

The X-29A (Fig. 1) incorporates many new technologies, the most evident of which is the forward-swept wing.⁸ The wing is made up of acroelastically tailored advanced composite wing skins which have been designed to avoid structural divergence and ensure structural integrity within the flight envelope. Dual hinged trailing-edge flaperons provide both aero-

dynamic camber and roll control. Directional control is provided by a conventional rudder. The variable incidence canards, wing flaperons, and strake flaps operate together to achieve minimum trim drag. The vehicle is statically unstable in pitch, with a negative static margin of up to 35 percent of the mean aerodynamic chord at subsonic speeds and does not achieve neutral stability until speeds of approximately Mach 1.4.

Flight-Control System

The flight-control laws for high-angle-of-attack flight are similar to those of the basic design described in reference 9 for flight up to 10° angle of attack. The high-angle-of-attack flight-control laws contain modifications for flight above 10° angle of attack.¹⁰

This section provides a brief description of the high-angle-of-attack FCS lateral-directional axis, since it was this axis in which the ASE interaction was observed. Figure 2 is a simplified schematic of the lateral-directional control laws. The high-angle-of-attack lateral-directional flight-control laws use only the roll rate and yaw rate sensors for feedback signals above 10° angle of attack. Below 10° angle of attack lateral acceleration is also used as a feedback sensor.

The flight-control law gains are various functions of dynamic pressure, Mach number, altitude, and angle of attack. The flight-control computer (FCC) updates surface commands at a rate of 40 Hz. All of the sensor paths have anti-aliasing filters while only the lateral acceleration and the yaw rate paths have additional notch filters. The notch filters were provided for attenuation of the feedback signals at the critical structural resonant frequency of 11 Hz. The entire low-angle-of-attack envelope ($\alpha < 20$, $M \leq 1.48$, $h \leq 52,000$ ft) was cleared without the need for a notch filter in the roll rate path.

Instrumentation

The aircraft instrumentation which helped detect the interaction consisted of the structural accelerometers and flight-control system (FCS) parameters (rate gyros, lateral accelerometers, actuator commands, and position signals). The locations of the structural accelerometers and rate gyros are shown in Fig. 3. A digital data bus provided access to the flight-control computer commands and feedback path signals. The feedback signals were analyzed at the point after the analog signal is digitized and the command signals

were analyzed at the point before the signal is converted from digital to analog (D/A) (Fig. 2). The sample rate was 400 samples/sec for the structural accelerometers and was 40 samples/sec for the FCS parameters.

Flight Conditions and Data Analysis

The analyzed flight conditions were 1-g flight envelope expansion test points for angles of attack from 10 to 45°. The entry speed for the high-angle-of-attack maneuvers was between 120 and 140 knots equivalent airspeed (KEAS). Higher entry speed maneuvers of 160 and 200 KEAS were also evaluated during the X-29A research. Entry altitude was 38,000 ft with an altitude loss of 5,000 to 13,000 ft occurring during the test maneuver. The minimum recovery altitude was 25,000 ft. The flight-control feedback gains were primarily a function of dynamic pressure and angle of attack which remained relatively constant during the maneuvers.

During the high-angle-of-attack flight maneuvers, the aircraft structure was being excited by the forebody vortices impinging on the vertical stabilizer. The wing also experienced separated flow for angles of attack greater than 15°, which added to the excitation. This excitation will be referred to as buffet.

The flight data were analyzed using fast Fourier transform (FFT) routines to obtain power spectrum densities (PSDs) of the vertical stabilizer structural accelerometers, the rate gyros, actuator commands, and surface position signals. The PSDs were used to find the frequency content of the signals and to determine the modal power in the frequency range of concern. The modal power was determined by amplitude summation of the data in a frequency range from 10 Hz to 20 Hz, in other words an integration of the area under the PSD curve. The modal power values from selected structural accelerometers and the rudder and flap position sensors were determined for each angle of attack flown in the range of 10 to 45° angle of attack. These data were plotted against angle of attack to show effects of the increased structural mode interaction as the aircraft flew at increasingly higher angles of attack.

Discussion of the Interaction

A structural interaction on the X-29A aircraft was observed during high-angle-of-attack flight testing. Aerodynamic buffet excited the aircraft's structural

modes at 11, 13, and 16 Hz, thereby causing signals at these frequencies to be measured by the roll rate and yaw rate gyros. The rate gyro output signals were then amplified through the flight-control laws and sent to the flaperons and rudder as additional commands.

Figure 4 is a flowchart showing structural interaction. The flowchart follows the interaction from the aircraft's response caused by the buffet through the flight-control system to the aircraft's control surfaces. Each aspect of the interaction will be discussed in the following sections using data from selected structural accelerometers and feedback sensors. All the PSDs shown are at an angle of attack of 30°, which was the angle of attack at which the buffet amplitudes peaked and started to level off.

Aerodynamic Buffet and the Aircraft Elastic Structural Response

As the aircraft's angle of attack increased, the intensity of the buffet on the vertical tail also increased. The increased buffet intensity caused an increase in the structural dynamic response of the airframe. This increase in dynamic response with angle of attack is shown by the modal power plots for selected structural accelerometers in Fig. 5. Increases in the airspeed also added greatly to the dynamic response as shown in the accelerometer data Fig. 6. In Fig. 5, the modal power increases approximately one and one-half orders of magnitude between 10 and 30° angle of attack but remains fairly constant from 30 to 45° angle of attack. Also shown is that the vertical stabilizer dynamic response is greater than that of the wing tips. Figure 6 shows that the accelerometers on the vertical stabilizer were responding more to the increased buffet at the higher speeds than the wing tips and flaperons.

A PSD of the rudder trailing-edge structural accelerometer signal at 30° angle of attack is shown in Fig. 7. There are three major structural response frequencies in the data. The first two are at 11 and 13 Hz and their response levels are approximately one order of magnitude greater than the noise floor. The third peak is at 16 Hz with a response level two orders of magnitude greater than the noise floor. From the ground vibration test of the X-29A,¹¹ the 11-Hz mode had been identified as an antisymmetric wing bending, the 13-Hz mode as a fuselage lateral bending, and the 16-Hz mode as vertical stabilizer bending. These

structural frequencies were also observed in the data from other structural accelerometers on the aircraft.

Flight-Control Sensor Feedback and Flight-Control System

As a result of the increased buffet on the aircraft, the roll and yaw rate gyros also sensed the structural modes. The PSDs of the rate gyro outputs (Fig. 8) show a high amplitude roll rate feedback between 10 and 20 Hz with the structural response peaks at 11, 13, and 16 Hz. The yaw rate signal over the same frequency band and flight conditions is approximately three orders of magnitude less and does not appear to be significant, which may be partially attributed to the additional notch filter at 11.2 Hz in the yaw rate path. The flowchart in Fig. 4 shows that the output from the rate gyros is sent through the flight-control system where the flight-control laws amplify the signal, then send it out as commands to the actuators.

Control Surface Actuator Command

The high amplitude roll rate feedback signal is now being commanded to the rudder and flaperon surfaces by the FCS. The PSDs of the flight-control computer commands to the rudder and flaperon channels are shown in Fig. 9. The rudder and flaperon command PSDs along with the roll rate signal PSD (Fig. 8) show similar frequency content. The structural resonant frequencies at 11, 13, and 16 Hz are apparent and the modal power trends are similar to the aircraft structural accelerometers shown in Fig. 5.

Rudder and Flap Actuators

The roll-off characteristics of the rudder and flap actuators, coupled with the rotational inertias of the control surfaces, tend to attenuate much of the actual control surface response at the high frequencies. The PSDs of the rudder and outboard flap position, shown in Fig. 10, still retain control surface response to the high frequency commands between 10 and 20 Hz. The resonant frequencies at 11, 13, and 16 Hz are again apparent. The relative amplitude of the position signal is approximately two orders of magnitude less than the amplitude of the commanded signals in this frequency band (Fig. 9). At and above 30° angle of attack the rudder and flaperon displacement were from ± 0.2 to $\pm 0.4^\circ$ shown by the modal powers in Fig. 11.

Surface Motion Induced Unsteady Aerodynamics

The small displacements of the rudder and flaperon would slightly affect the unsteady aerodynamics. This displacement would only produce a small amount of additional structural excitation because of the small rotational inertias of the control surfaces. In addition, the control surface effectiveness is reduced because of the low dynamic pressure flight conditions which again result in little structural excitation. The control surface-induced unsteady aerodynamic excitation was washed out by the high buffet excitation on the aircraft. As a result, the aerodynamics which are needed to sustain or cause a limited amplitude oscillation of the vertical stabilizer are not present in the interaction. The absence of the aerodynamics creates an open-loop situation which means that the path represented by the dotted line in Fig. 4 is negligible in this case.

Consequences of the Interaction

Although this interaction did not produce an instability, an adverse effect of the feedback interaction occurred during the higher speed maneuvers while the aircraft was flying at 30° angle of attack or above. The servoactuator was reconfigured and a servoactuator failure annunciator light was illuminated during the flight-test point, caused in part by the increased surface activity as shown in Fig. 6. A schematic of the servoactuator hydraulic system is shown in Fig. 12. Each actuator, controlled by three independent servovalves, operates one surface. Each servovalve receives a signal from one of the three FCCs. The hydraulic output from the servovalves is sent to a hydraulic voting block to compare the three outputs. If the servovalve output pressures agree within the specified limits, the average signal from servovalve one and two is used as the command to the actuator power ram (S1 is closed in Fig. (12)). If any of the servovalve output pressures do not agree, the servoactuator is reconfigured and a warning light is illuminated in the cockpit. An error in servovalve 1 or servovalve 2 results in a reconfiguration consisting of using the signal from servovalve 3 to generate actuator commands (S2 is closed in Fig. (12)).

The high-amplitude roll rate signal commands in the 10- to 20-Hz frequency range may have caused the servoactuator reconfiguration. These high-frequency

commands were outside the actuator's response capability. The first servovalve failure caused the flight test to be terminated. In later flights, the actuators were reset inflight, and the point was repeated until it was successfully flown without a servovalve failure indication. The long-term effects of the commanded high frequency signals on the actuators is unknown at this time.

A notch filter was designed and implemented for the roll rate gyro path of the flight-control system (Fig. 2). The roll-off characteristics of the actuator system of the X-29A prevented this ASE interaction from becoming a limited amplitude oscillation or an ASE instability.

Concluding Remarks

An aerostructural interaction was observed in the lateral-directional axis of the flight-control system during the high-angle-of-attack flight envelope expansion of the X-29A forward-swept wing aircraft. The interaction consisted of an 11-, 13-, and 16-Hz structural mode being excited by high buffet levels, fed through the flight-control system, and then commanded to the control surface actuators. There was a small magnitude aerodynamic excitation which was induced by the control surface movement. The effects of the excitation were washed out by the high level of buffet excitation on the aircraft. The result of the excitation was that this ASE interaction did not result in a closed-loop instability or a limited amplitude oscillation.

The control surface actuators could not fully respond to the high frequency commands induced by the ASE interaction. This contributed to redundancy management (hydraulic logic) miscompares between the servovalve output pressures and to servoactuator reconfiguration. This servoactuator failure indication resulted in an increase of flight-test time and maneuvers to clear the desired high-angle-of-attack flight envelope safely. These ASE interactions were catalysts for changes in the flight-control system including the addition of a notch filter to the roll rate gyro path.

References

¹Barfield, A. Finley, and Felt, Larry R., "Aeroservoelasticity—A Merging of Technologies,"

Society of Flight Test Engineers 7th Annual Symposium, Eastsound, WA, Aug. 4–6, 1976.

²Gupta, K.K., Brenner, M.J., and Voelker, L.S., "Integrated Aeroservoelastic Analysis Capability with X-29A Comparisons," *J. of Aircraft*, vol. 26, no. 1, Jan. 1989, pp. 84–90.

³Peloubet, R.P., Jr., Haller, R.L., Cunningham, A.M., Cwach, E.E., and Watts, D., "Application of Three Aeroservoelastic Stability Analysis Techniques," AFFDL-TR-76-89, Air Force Flight Dynamics Laboratory, Wright-Patterson Air Force Base, OH, Sept. 1976.

⁴Zislin, A., Laurie, E., Wilkinson, K., and Goldstein, R., "X-29 Aeroservoelastic Analysis and Ground Test Validation Procedures," AIAA-85-3091, AIAA/AHS,ASEE Aircraft Design Systems and Operations Meeting, Colorado Springs, CO, Oct. 1985.

⁵Kehoe, Michael W., Laurie, Edward J., and Bjarke, Lisa J., *An In-Flight Interaction of the X-29A Canard and Flight Control System*, NASA TM-101718, 1990.

⁶Peloubet, R.P., Jr., "YF-16 Active-Control-System/Structural Dynamics Interaction Instability," AIAA-75-823, AIAA/ASME/SAE 16th Structures, Structural Dynamics, and Materials Conference, Denver, CO, May 1975.

⁷Kehoe, Michael W., *AFTI/F-16 Aeroservoelastic and Flutter Flight Test Program—Phase I*, NASA TM-86027, 1985.

⁸Chacon, Vince, and McBride, David, *Operational Viewpoint of the X-29A Digital Flight Control System*, NASA TM-100434, 1988.

⁹Whitaker, A., and Chin, J., "X-29 Digital Flight Control System Design," AGARD-CP-384, Oct. 1984.

¹⁰Pellicano, Paul, Krumenacker, Joseph, and Vanhoy, David, "X-29 High Angle-of-Attack Flight Test Procedures, Results, and Lessons Learned," Society of Flight Test Engineers 21st Conference, Garden Grove, CA, Aug. 6–9, 1990.

¹¹Flynn, J., and Dilea, J., "Results of the Ground Vibration Survey of the X-29A No. 2 Aircraft with Spin Chute Installation," GASD Report X-29-380-TR-8802, Grumman Aerospace Corporation, Bethpage, NY, Oct. 1988.

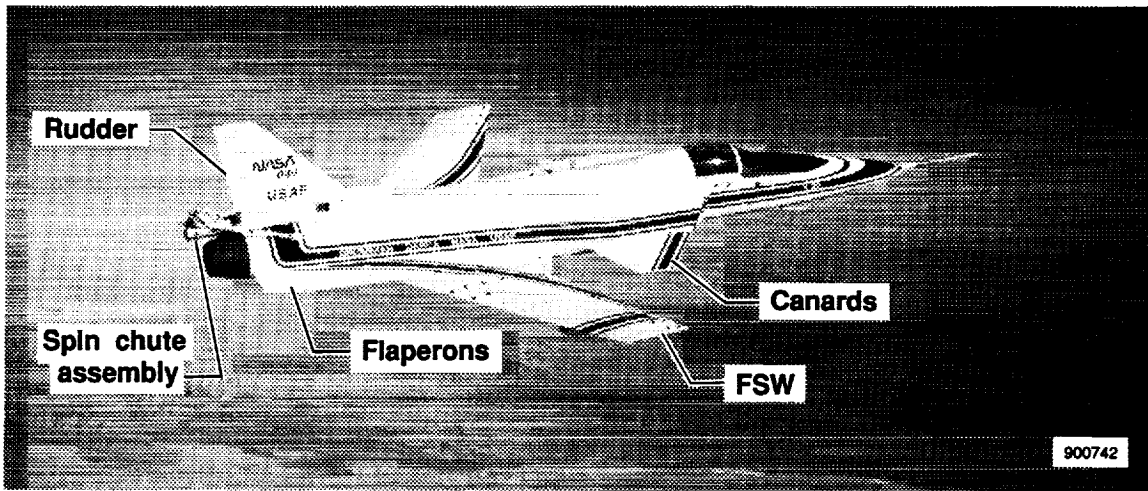
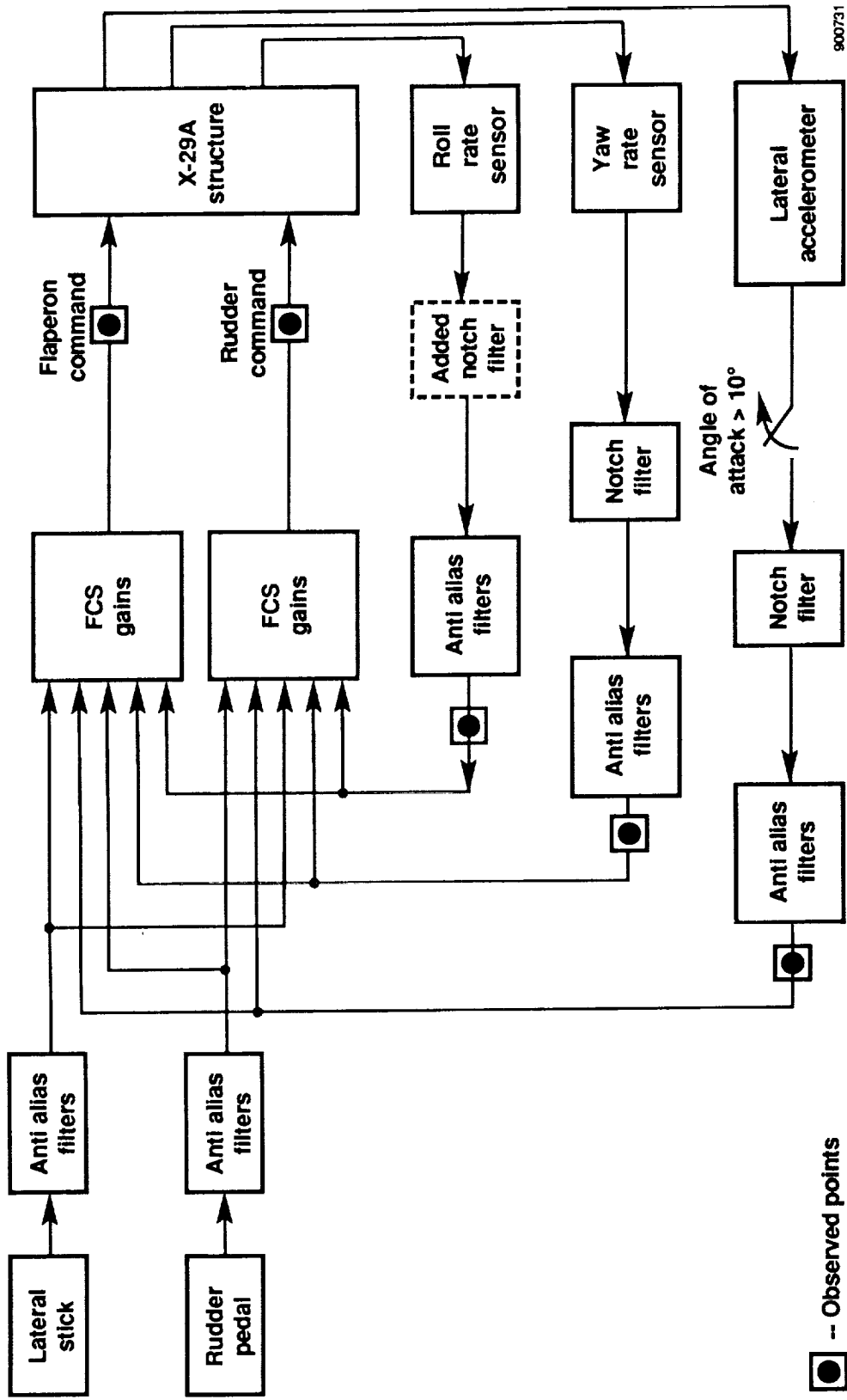


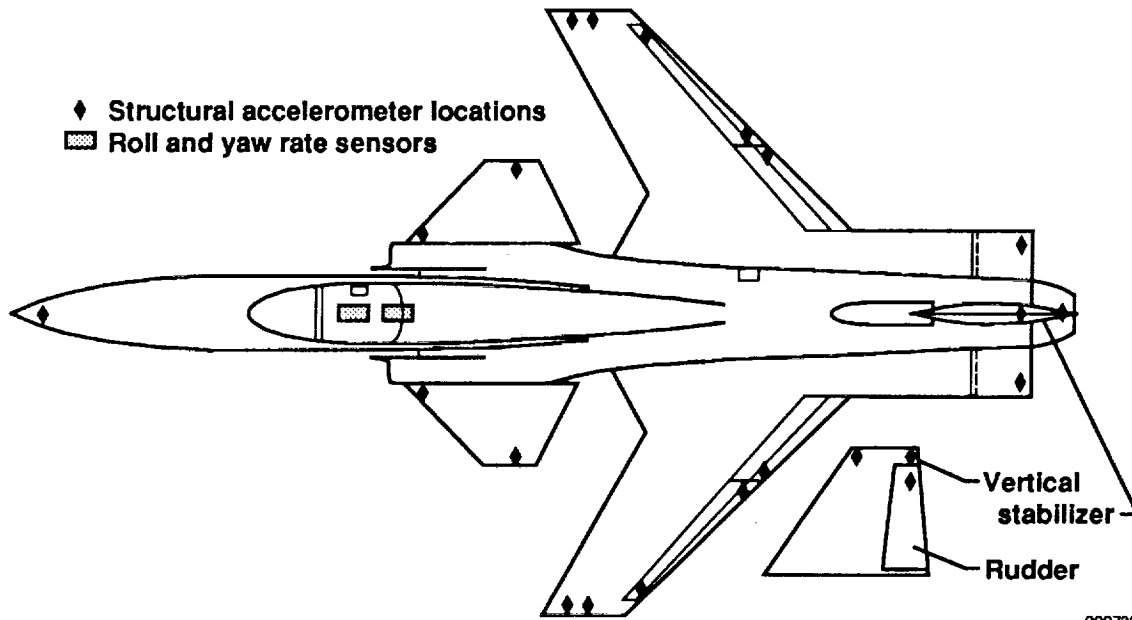
Figure 1. X-29A forward-swept wing aircraft.

ORIGINAL PAGE IS
OF POOR QUALITY



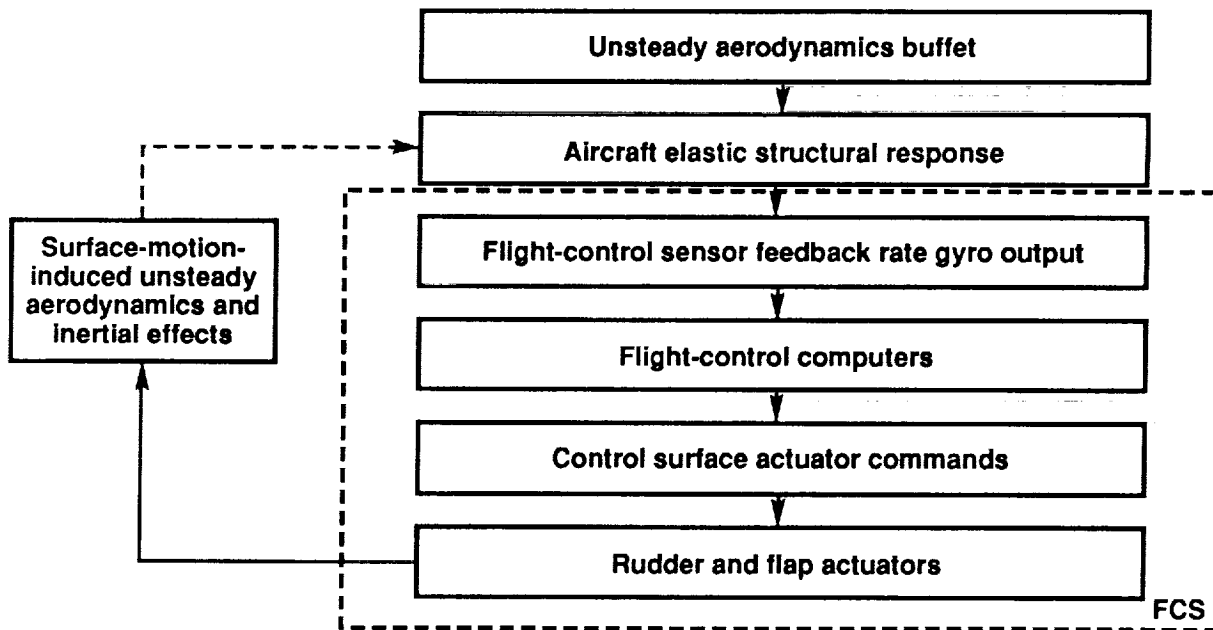
900731

Figure 2. Simplified lateral-directional flight-control law block diagram for high-angle-of-attack flight.



900732

Figure 3. Accelerometer and rate sensor locations.



900733

Figure 4. Structural interaction flowchart.

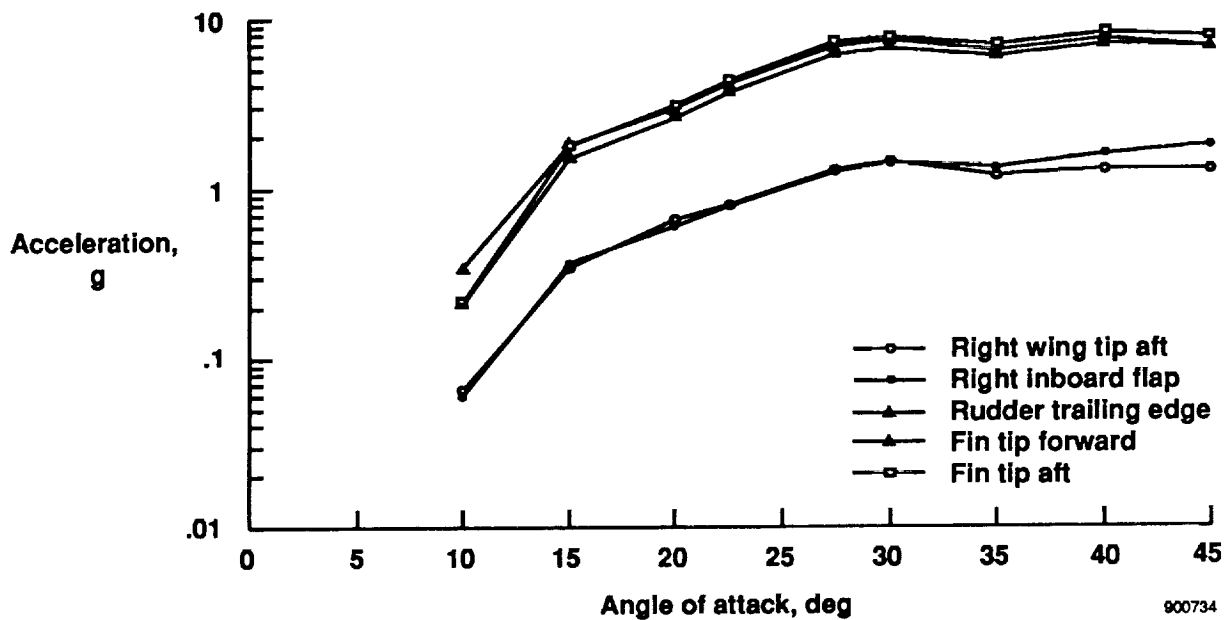


Figure 5. Modal power trends in aircraft structural accelerometers.

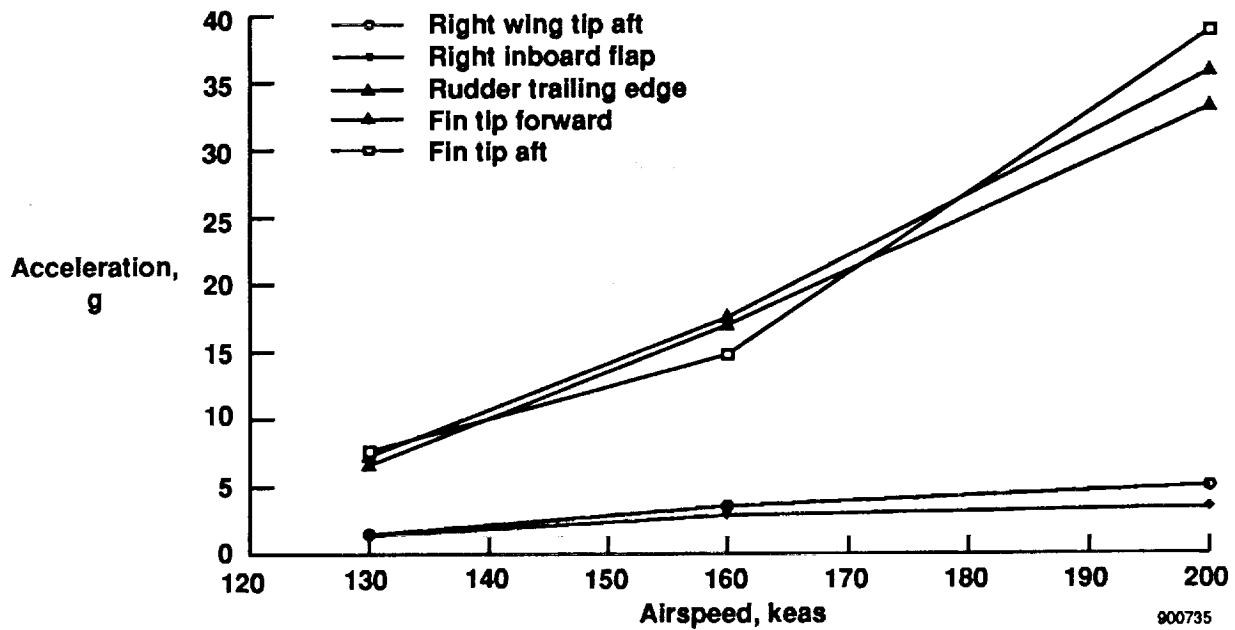


Figure 6. Modal power trends with airspeed in aircraft structural accelerometers.

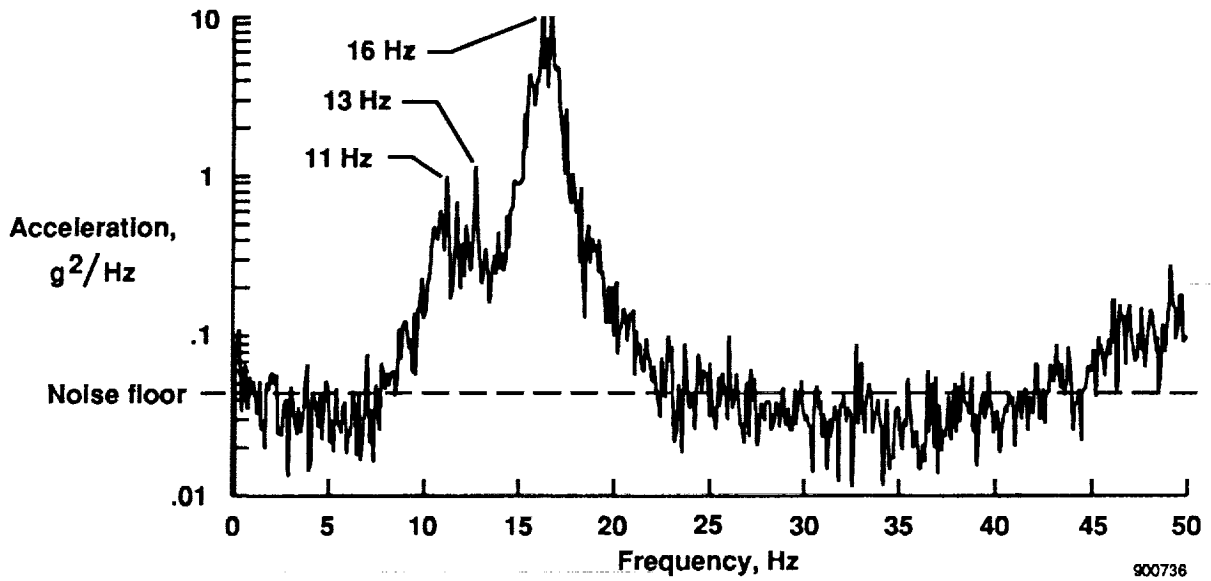


Figure 7. Power spectral densities of rudder accelerometer.

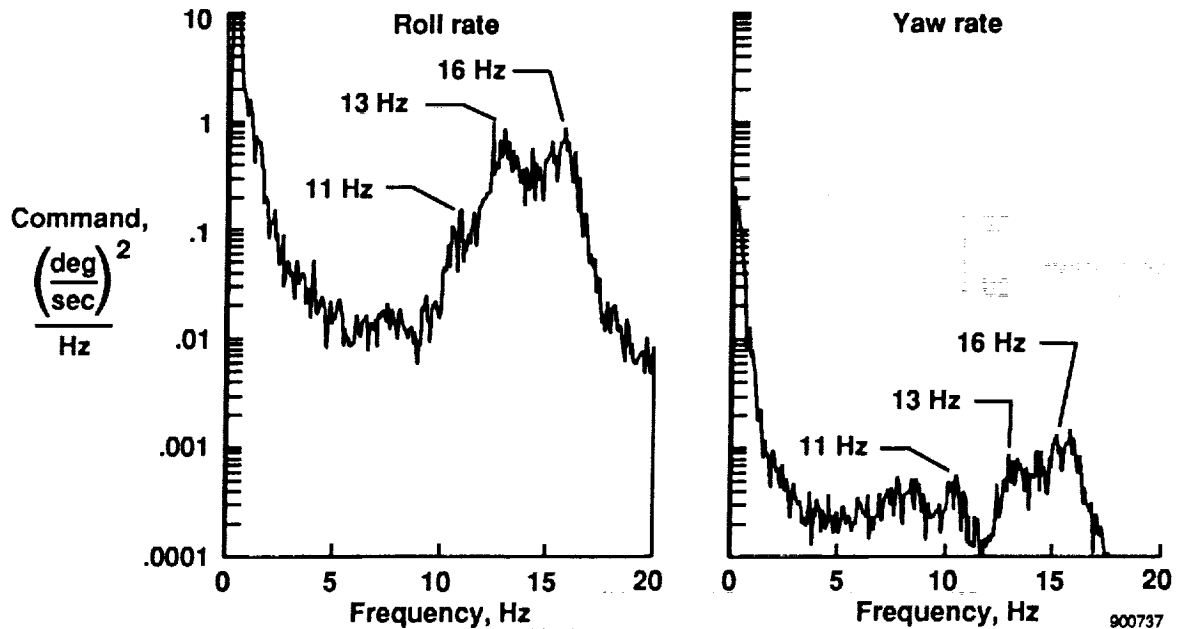


Figure 8. Power spectral densities of roll rate and yaw rate feedback sensor.

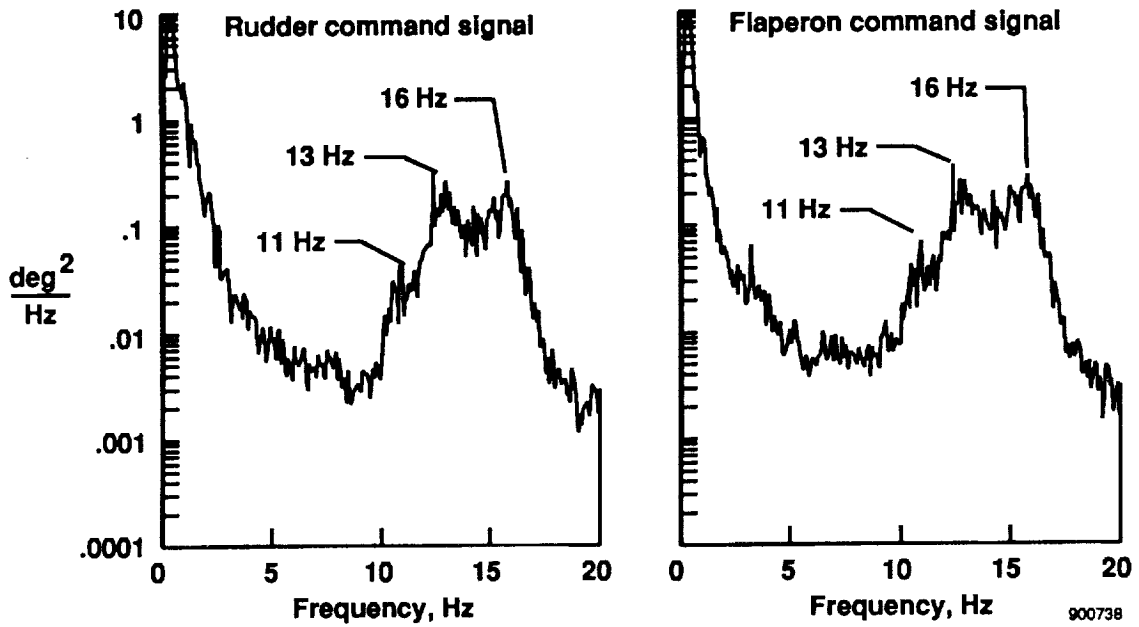


Figure 9. Power spectral densities of rudder and flaperon actuator commands.

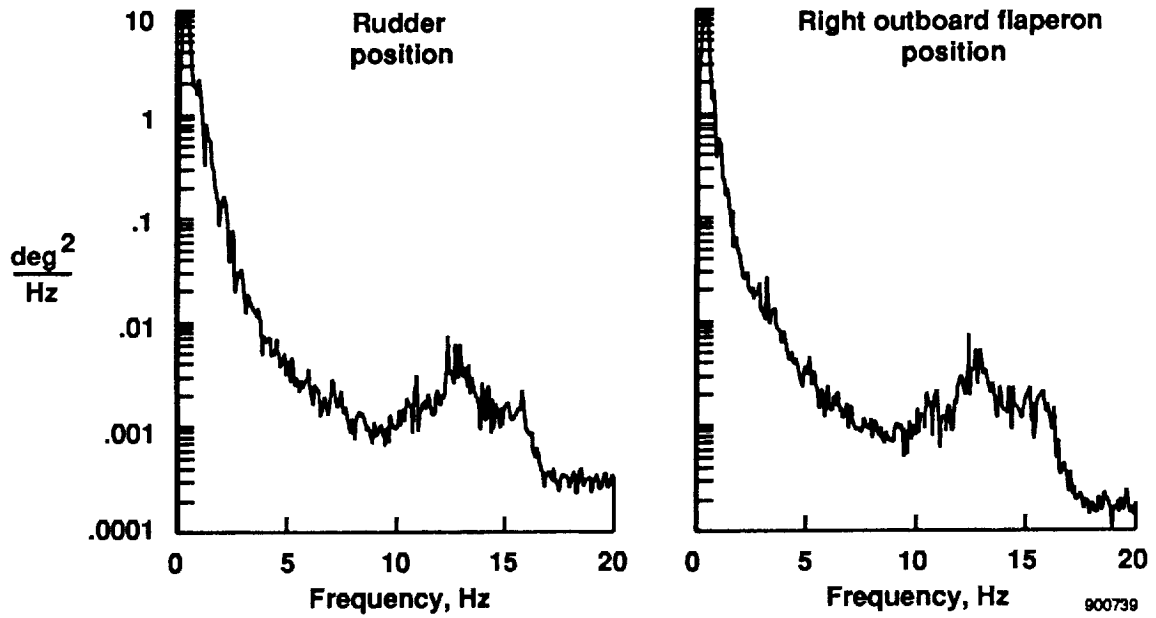


Figure 10. Power spectrums of rudder and flaperon positions.

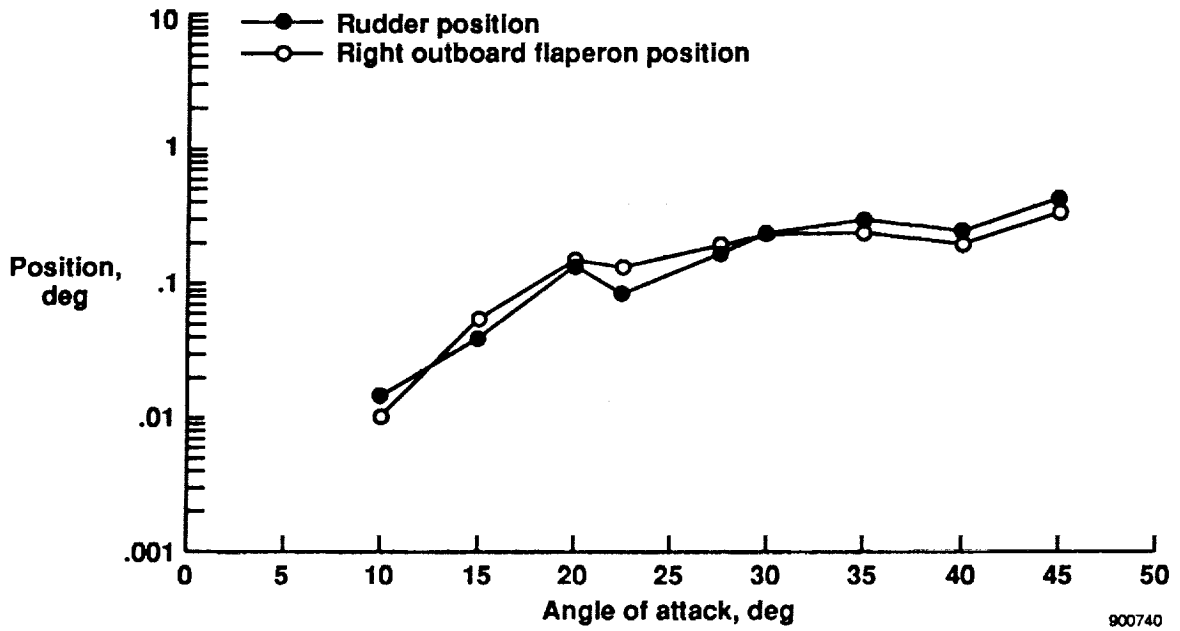


Figure 11. Power spectral densities of rudder and flaperon positions.

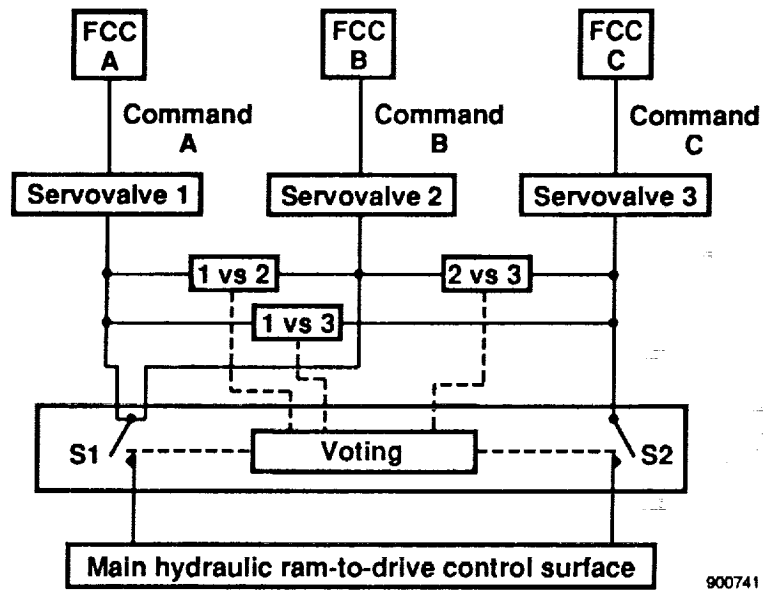


Figure 12. Servoactuator hydraulic schematic.



Report Documentation Page

| | | | | | |
|---|--|--|---|---|------------------|
| 1. Report No. NASA TM-101735 | | 2. Government Accession No. | | 3. Recipient's Catalog No. | |
| 4. Title and Subtitle Buffet Induced Structural/Flight-Control System Interaction of the X-29A Aircraft | | | | 5. Report Date April 1991 | |
| | | | | 6. Performing Organization Code | |
| 7. Author(s) David F. Voracek and Robert Clarke | | | | 8. Performing Organization Report No. H-1687 | |
| | | | | 10. Work Unit No. RTOP 533-02-51 | |
| 9. Performing Organization Name and Address NASA Ames Research Center Dryden Flight Research Facility P.O. Box 273, Edwards, California 93523-0273 | | | | 11. Contract or Grant No. | |
| | | | | 13. Type of Report and Period Covered Technical Memorandum | |
| 12. Sponsoring Agency Name and Address National Aeronautics and Space Administration Washington, DC 20546-3191 | | | | 14. Sponsoring Agency Code | |
| | | | | | |
| 15. Supplementary Notes Presented as paper #91-1053 at the 32nd AIAA Structures, Structural Dynamics, and Materials Conference, April 8-10, 1991, Baltimore, Maryland. | | | | | |
| 16. Abstract High-angle-of-attack flight regime research is currently being conducted for modern fighter aircraft at the NASA Dryden Flight Research Facility. This flight regime provides enhanced maneuverability to fighter pilots in combat situations. Flight research data are acquired to compare and validate advanced computational fluid dynamic solutions and wind-tunnel models. High-angle-of-attack flight creates unique aerodynamic phenomena including wing rock and buffet on the airframe. These phenomena increase the level of excitation of the structural modes, especially on the vertical and horizontal stabilizers. With high gain digital flight-control systems, this structural response may result in an aeroservoelastic interaction. A structural interaction on the X-29A aircraft was observed during high-angle-of-attack flight testing. The roll and yaw rate gyros sensed the aircraft's structural modes at 11, 13, and 16 Hz. The rate gyro output signals were then amplified through the flight-control laws and sent as commands to the flaperons and rudder. The flight data indicated that as the angle of attack increased, the amplitude of the buffet on the vertical stabilizer increased, which resulted in more excitation to the structural modes. The flight-control system sensors and command signals showed this increase in modal power at the structural frequencies up to 30° angle of attack. Beyond 30° angle of attack, the vertical stabilizer response, the feedback sensor amplitude, and control surface command signal amplitude remained relatively constant. Data are presented that show the increased modal power in the aircraft structural accelerometers, the feedback sensors, and the command signals as a function of angle of attack. This structural interaction is traced from the aerodynamic buffet to the flight-control surfaces. | | | | | |
| 17. Key Words (Suggested by Author(s)) X-29A aircraft High Angle of Attack Buffet Aeroservoelasticity | | | 18. Distribution Statement Unclassified-Unlimited Subject category 05 | | |
| 19. Security Classif. (of this report) Unclassified | | 20. Security Classif. (of this page) Unclassified | | 21. No. of Pages 12 | 22. Price A02 |

1
2
3
4
5
6
7
8
9
10
11
12
13
14
15
16
17
18
19
20
21
22
23
24
25
26
27
28
29
30
31
32
33
34
35
36
37
38
39
40
41
42
43
44
45
46
47
48
49
50
51
52
53
54
55
56
57
58
59
60
61
62
63
64
65
66
67
68
69
70
71
72
73
74
75
76
77
78
79
80
81
82
83
84
85
86
87
88
89
90
91
92
93
94
95
96
97
98
99
100